Available online at www.sciencedirect.com
ScienceDirect
Journal of Power Sources 175 (2008) 826–832
JOURNAL OF POWER SOURCES
www.elsevier.com/locate/jpowsour

Application of hyperdispersant to the cathode diffusion layer for direct methanol fuel cell

Qing Mao [a,b], Gongquan Sun [a,*], Suli Wang [a], Hai Sun [a], Yang Tian [a,b], Juan Tian [a,b], Qin Xin [a]

[a] *Direct Alcohol Fuel Cell Laboratory, Dalian Institute of Chemical Physics, CAS, Dalian 116023, China*
[b] *Graduate School of the Chinese Academy of Sciences, Beijing 100039, China*

Received 2 September 2007; received in revised form 27 September 2007; accepted 27 September 2007
Available online 10 October 2007

Abstract

In this study, Nafion ionomer, as a kind of hyperdispersant, was added to polytetrafluoroethylene (PTFE) water dispersion system to suppress the size of PTFE particles in the ink of microporous layer (MPL). The agglomeration behavior of PTFE in ethanol and MPL were investigated by laser diffraction, dynamic light scattering (DLS) and metallurgical microscopes. The electronic resistance, pore size distribution, gas permeability and surface hydrophobic/hydrophilic properties were also characterized for prepared gas diffusion layers (GDLs). It was shown that PTFE water dispersion system suffered flocculating when dispersed in ethanol and this agglomeration behavior was reduced by employing Nafion ionomer. With the increase in the Nafion ionomer adopted in the MPL, not only the decreased hydrophobic property was shown in the MPL, but the decreased PTFE particle size was also achieved, which results in improved crosslink of carbon and pores themselves as well as the volume loss of pores in micron scale. The increased gas permeability and electronic conductivity of the GDL made the one employing the PTFE dispersion system with 1% Nafion content own its advantages as the cathode diffusion layer for a direct methanol fuel cell (DMFC) under near-ambient conditions.

Keywords: Polytetrafluoroethylene; Hyperdispersant; Agglomeration behavior; Gas diffusion layer; Water management; Direct methanol fuel cell

1. Introduction

Direct methanol fuel cell (DMFC) is attractive for the application of portable power sources due to its high-energy density and simple structure. The cell performance and stability at atmosphere pressure with relatively low air stoichiometry are widely regarded as the key issues for its potential commercialization. Under such a severe cathode operation condition, sufficient importance has been attached to the management of water and gas employed by the gas diffusion layer (GDL) in the cathode [1,2].

The cathode GDL, which is composed of support layer (carbon fiber paper or carbon cloth) and microporous layer (MPL), not only serves as a pathway for the diffusion of air to the cathode, but also as a conduit for the removal of the byproduct water from the cathode. It is reported that the MPL in the GDL can improve both the cell performance and stability due to its effective water management as measured and as modeled [3–7]. As a consequence, extensive experimental work has been done by many researchers to study the effect of the type and loading of carbon powder, the content of polytetrafluoroethylene (PTFE) as well as the adding of pore-forming agent in MPL on the cell performance. Park et al. [8] investigated how the carbon loading in the MPL affected the fuel cell performance. It was suggested that high loading of carbon would cause severe water flooding in the catalyst layer due to high-flow resistance. By contrast, low loading of carbon would result in water flooding in the support layer, thereby impeding oxygen diffusion in the GDL. Furthermore, Passalacqua et al. [9] prepared the MPLs using different types of carbon black. The observed performance improvement was attributed to higher pore volume and smaller pore size (1–10 μm in radius) of acetylene black. Park et al. [10] also introduced the wire-like carbon nano-fibers to carbon powder for MPL preparation. The increased gas permeability and

* Corresponding author. Tel.: +86 411 84379063; fax: +86 411 84379063.
E-mail address: gqsun@dicp.ac.cn (G. Sun).

0378-7753/$ – see front matter © 2007 Elsevier B.V. All rights reserved.
doi:10.1016/j.jpowsour.2007.09.111

electronic conductivity of the GDL was believed to contribute to the improvement of the cell performance. Kong et al. [11] further modified the MPL structure by pore-forming agent. Experimental results showed that the increased volume of macropores (5–20 μm in diameter) resulted in better performance. As for the hydrophilic/hydrophobic properties in the GDL, Kim et al. [2] proposed that the cathode diffusion layer should possess hydrophilicity and hydrophobicity at the same time. In the membrane electrode assembly (MEA), the hydrophilic ordered mesoporous silica was adopted in the cathode to reduce the water transport flux caused by the concentration gradient between the anode and the cathode. PTFE, as a kind of hydrophobic agent, is usually added to the MPL to increase its contact angle to water and prevent flooding in the cathode. According to Giorgi et al. [12], increased PTFE content in the MPL can decrease the total porosity and the volume of the pores whose radius are larger than 0.35 μm in the GDL. It was suggested that 10 wt.% PTFE in the MPL was required to avoid water flooding and improve the gas transport. However, excessive PTFE loading in the MPL was unfavorable to cell performance, which was mainly attributed to the decreased gas permeability in the cathode GDL [12–14].

As it is said above, it is clear that much attention has been focused on the issues of loading, morphology and structure, dispersion status and hydrophobic/hydrophilic properties, etc. of carbon powder. As for the other composition in the MPL, the content alteration of PTFE is the only way to realize the structural and properties' adjustment. As we know, even with the same carbon powder, the morphology and dispersion status of the PTFE also exerts strong influence on the pore structure and internal hydrophobic/hydrophilic properties in the MPL. But little work has been carried out in this regard.

In this study, Nafion ionomer, as a kind of hyperdispersant, was adopted to suppress the particle size of PTFE aggregation in the MPL ink. Dynamic light scattering (DLS), laser diffraction and metallurgical microscopes were used to identify the particle size of the PTFE in the MPL ink. The pore size distribution, gas permeability, electronic conductivity and surface contact angle were characterized for prepared GDLs to investigate the variation of the pore structure and hydrophobic/hydrophilic properties caused by the additional Nafion ionomer. Acting as the cathode GDLs, the corresponding effects of prepared GDLs on the DMFC performance was further investigated under near-ambient conditions.

2. Experimental

2.1. Characterization of PTFE aggregation behavior in ethanol and MPL

Five PTFE water dispersion systems (E1–E5) were prepared to characterize the agglomeration behavior of PTFE in water and ethanol, respectively. E1 was a diluted PTFE dispersion FR301B (3F New Material Co. Ltd.) with deionized (DI) water, whose concentration is 10 wt.%. And the samples E2–E5 were prepared by introducing Nafion ionomer into E1 with a concentration of 0.5 wt.%, 1 wt.%, 2 wt.% and 5 wt.%, respectively. The particle size distributions of the sample E1 in DI water and samples E1–E5 in ethanol were characterized by means of laser diffraction and DLS experiments. Laser diffraction was conducted by a laser particle sizer BT-9300 (Dandong, China), which used semiconductor laser ($\lambda = 635$ nm) and could detect the particle size distribution in the range of 0.1–340 μm. The DLS measurements were employed by a Malvern Zetasizer 3000 (Malvern Instruments), using a He–Ne laser light ($\lambda = 633$ nm) and a scattering angle of 90°. It provides a rapid detection of the size distribution in the range of 0.3–3000 nm.

Carbon paste of the MPL was prepared by mixing carbon black (acetylene black) with ethanol through simultaneous mechanical stir and sonication for 20 min. The MPL ink was obtained by introducing a PTFE dispersion sample into the carbon paste with mechanical stir for 20 min. The weight ratio of PTFE:ethanol:carbon (dry weight) in MPL ink is 1:50:1. Thereafter, the prepared MPL ink was dripped on the slide and dried out at room temperature for characterizing the surface morphology by Metallurgical Microscopes XJZ-6 (Jnoec Ltd.).

2.2. Preparation and characterization of the cathode GDLs

Toray carbon paper (TGP-H-030) was used as the support layer of the cathode GDL. In order to make it waterproofed, it was dipped entirely in 2 wt.% diluted PTFE water dispersion system and dried at room temperature repeatedly until 20 wt.% PTFE was loaded on. The MPL ink prepared with different PTFE water dispersion system was then applied to the support layer with doctor blade technique. And then, the samples were sintered in air at 340 °C for half an hour. The carbon loading in the GDLs is 4.4 ± 0.1 mg cm^{-2}, which is the optimized value for the cathode GDL. The obtained GDLs (GDL1–GDL4) and the employed PTFE water dispersion systems are listed in Table 1.

Gas permeability through a GDL was measured using the laboratory fabricated apparatus which is same as that shown in the literature [15]. The flow rate of nitrogen through a GDL in the through-plane direction and the pressure drop across the GDL were both measured. The permeability coefficient, which represents the gas permeability of a sample, was then calculated

Table 1
Main characteristic of the GDL samples

Cathode GDL no.	GDL1	GDL2	GDL3	GDL4
PTFE dispersant	E1	E3	E4	E5
Thickness (μm)	320.0	310.7	309.2	281.3
Gas permeability (m^2)	5.2E−12	2.1E−12	7.3E−13	5.5E−13
Total mercury intrusion (mL g^{-1})	1.1238	1.1728	1.1801	0.8770
Mercury intrusion (1–7.3 μm) (mL g^{-1})	0.1769	0.1629	0.1529	0.0480
Mercury intrusion (0.05–1 μm) (mL g^{-1})	0.7401	0.7705	0.8052	0.6716
Resistance of GDL (mΩ cm^2)	28.2	24.6	21.2	11.9
Contact angle (°)	148.5	146	144.5	144

basing on a rearranged form of Darcy's law [16].

$$k = \upsilon\mu\frac{\Delta X}{\Delta P} \quad (1)$$

where k is the permeability coefficient of a porous substrate, m^2; υ the superficial velocity, calculated from the nitrogen flow rate divided by the area of a sample, $m\,s^{-1}$; μ the fluid viscosity 1.8×10^{-5} Pa for nitrogen at 23 °C; ΔX the thickness of a substrate, m; and ΔP is the pressure drop across a substrate, Pa. To calculate gas permeability coefficient of all the GDLs, the thickness of each, listed in Table 1, was measured using a micrometer. The area of each sample is 3.0 cm × 3.0 cm.

In through-plane direction, electronic resistance of the GDL was measured by chronopotentiometry method by a bipolar power supply PBX 20–20 (KIKUSUI). The area of each sample is 2.5 cm × 2.5 cm.

Internal pore structure information of the GDLs was obtained by MIP (Quantachrome Pore Master 60), which measured the amount of penetrated mercury as a function of the applied pressure. The value of mercury surface tension is 4.8×10^{-3} N cm^{-1} and the contact angle of mercury on the sample surface is 140°.

Surface hydrophobicity/hydrophilicity of the GDLs were investigated by contact angle measurements. The measurements were carried out with a contact angle meter (JC2000A, Powereach Instruments) at 20 °C. The sample was placed on a sample table and a droplet of water was dripped on the sample with a syringe. As soon as we dripped a droplet of water on the sample, images of the droplet were taken with a digital camera and the fitted curves of the edge of the droplet were used to calculate the values of the contact angle.

2.3. Preparation and characterization of the MEAs

The carbon paper TGP-H-060 and the MPL ink with PTFE dispersion E1 was adopted for preparing anode diffusion layer through above methods. The carbon loading of the MPL is 2.0 mg cm^{-2}.

Unsupported PtRu black (Johnson Matthey HiSpec 6000, Pt:Ru = 1:1 atomic ratio) and Pt/C (Johnson Matthey HiSpec 9100, 60 wt.%) were used as anode and cathode catalyst, respectively. The mixture of DI water, catalyst powder and Nafion ionomer were sonicated in an ice bath for 40 min. According to in-house optimized results of preparing methods under near-ambient conditions [17], the anode catalyst ink was deposited on the diffusion layer by brush painting method and the cathode catalyst ink was applied on the membrane by spraying method. Numerous thin coats of the catalyst ink were successively applied onto the substrate at 60 °C for both the above methods and each coat was dried for 2 min before another coat was deposited on. The catalyst loadings of the anode and the cathode catalyst layers in this paper are 7.4 mg PtRu cm^{-2} and 1.9 ± 0.1 mg Pt cm^{-2}, respectively. The ratio of catalyst to Nafion ionomer is maintained to be 7.67:1 (dry weight) for both anode and cathode catalyst layers. Nafion®-1135 (E.I. DuPont de Nemours and Company) membrane was used as the electrolyte for all the MEAs. Cathode gas diffusion layers GDL1–GDL4 were adopted in the cell C1–C4, respectively. Without lamination, each compartment of a cell was assembled between two stainless steel plates with a serpentine flow field. The active area of the cell is 4.0 cm^2.

The polarization curves were obtained using a Fuel Cell Test System (Arbin Instrument Corp.) under the operation conditions of 80 °C, 0.5 mol L^{-1} methanol aqueous solution with a flow rate of 1 mL min^{-1} in the anode and dried air with volume flow rate of 80 mL min^{-1} in the cathode. The total ohmic loss of the methanol/air cell was measured by the current interruption technique.

The steady-state anode potentials were obtained from the IR-corrected anode polarizations, which were measured by EG&G PAR 273A potentionstat/galvanostat at 80 °C. The anode compartment was supplied with 0.5 mol L^{-1} methanol aqueous solution serving as the working electrode. The cathode was fed with humidified H_2 at 80 °C, acting as the counter electrode and the dynamic hydrogen reference (DHE). The resistance of methanol/H_2 cell was measured by electrochemical impendence spectroscopy (EIS). The steady-state cathode potential was calculated from the sum of the IR corrected cell voltage and anode potential.

3. Results and discussion

3.1. Agglomeration behavior of PTFE in ethanol solution

Fig. 1 shows the particle size distribution of E1 diluted by DI water and that dispersed in ethanol measured by laser diffraction technique. It is shown that the medium diameter (D50) of the PTFE is 0.26 μm when dispersed in DI water. In the ethanol, PTFE suffers severe flocculating. The D50 increases to 31.23 μm when a PTFE content is 0.27 wt.%. As the concentration of PTFE increases to 0.35 wt.% and 0.42 wt.%, the D50 increases to 40.52 μm and 47.30 μm, respectively. However, the agglomeration behavior of PTFE in ethanol is reduced

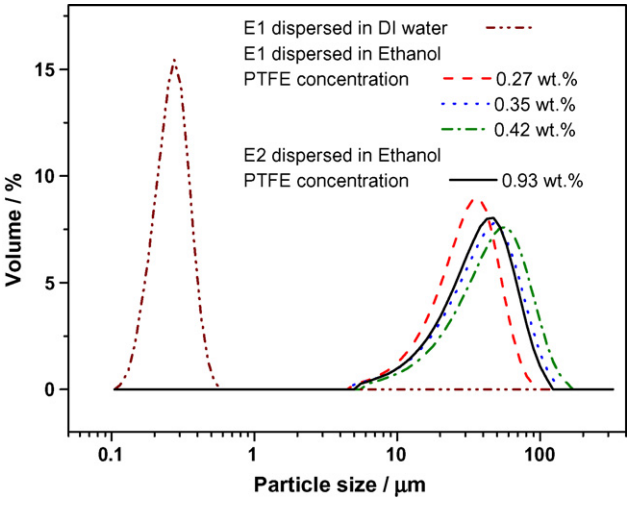

Fig. 1. Particle size distribution of PTFE water dispersion system E1 and E2 dispersed in DI water and ethanol measured by laser diffraction.

when Nafion ionomer is added to PTFE water dispersion system. The D50 of dispersant E2 is 38.48 μm when PTFE content increases to 0.93 wt.%.

Fig. 2 shows the particles size distribution measured by DLS technique. Being different from laser diffraction technique, DLS measures the time-dependent intensity fluctuations of scattered light for a suspension of particles which only undergo random, Brownian motion. As shown in Fig. 2(a), the mean particle size of PTFE dispersant E1 is 0.255 μm, which is in accordance with that measured by laser diffraction. When it was dispersed in ethanol, the mean value of PTFE particle is reduced to 0.207 μm (Fig. 2(b)). The particle size distributions of the PTFE dispersant with certain concentration of Nafion ionomer are also presented in Fig. 2(c–e). The mean particle size is 0.210 μm for the PTFE dispersion with 1 wt.% Nafion being dispersed in ethanol. When the concentration of Nafion increases to 2 wt. % and 5 wt. %, the mean particle size is 0.237 μm and 0.266 μm, respectively.

It is reported that the nonionic surfactants such as "Triton X-100" are used as the stabilizer in the PTFE water dispersion system [18]. The nonionic surfactant can resist the particles agglomerating by the steric stabilization in PTFE water dispersion system. Comparing with water, ethanol has lower dielectric constant and smaller dipolar moment. The additive ethanol decreases the polar character of the medium, which entails more difficulties for both micellization and phase separation of the PTFE [19]. Therefore, the dispersion stability of the original surfactant to PTFE in ethanol is less than that in water. The release of the original surfactant and consequent flocculating of PTFE in ethanol are confirmed by reduced PTFE particle size measured by DLS and increased PTFE particle size measured by the laser diffraction, respectively.

Polymeric hyperdispersants have been adopted to improve the pigment dispersion in nonaqueous solvent [20]. Anchoring group and the polymeric chains are the two key components in the structure of the hyperdispersant. In organic medium, the forming process of steric stabilization can be explained by the entropic changes when two particles approach. The free movement of the polymeric chains is reduced as the chains intermingle, and such a state is unfavorable for the free energy terms, therefore the chains (and therefore the enclosed PTFE particles) move apart to a more preferred state. Nafion ionomer is a typical 'COMB' copolymer [21], which has the characteristics of hyperdispersants. Sulfonate radical is a typical anchoring group and the fluorocarbon chain has enough molecular weight to serve as the steric barrier.

Fig. 2(f) shows the particle size distribution of the Nafion ionomer dispersed in ethanol. The mean value of Nafion particle diameter is 0.847 μm. However, there are not two characteristic peaks when the mixture of Nafion and PTFE dispersed in ethanol. It is indicated that Nafion ionomer is easier to adsorb on the PTFE surface in ethanol. With the increase in the Nafion ionomer content, the particle size increases, which suggest that Nafion ionomer continue to adsorb through the interaction force between the Nafion ionomers.

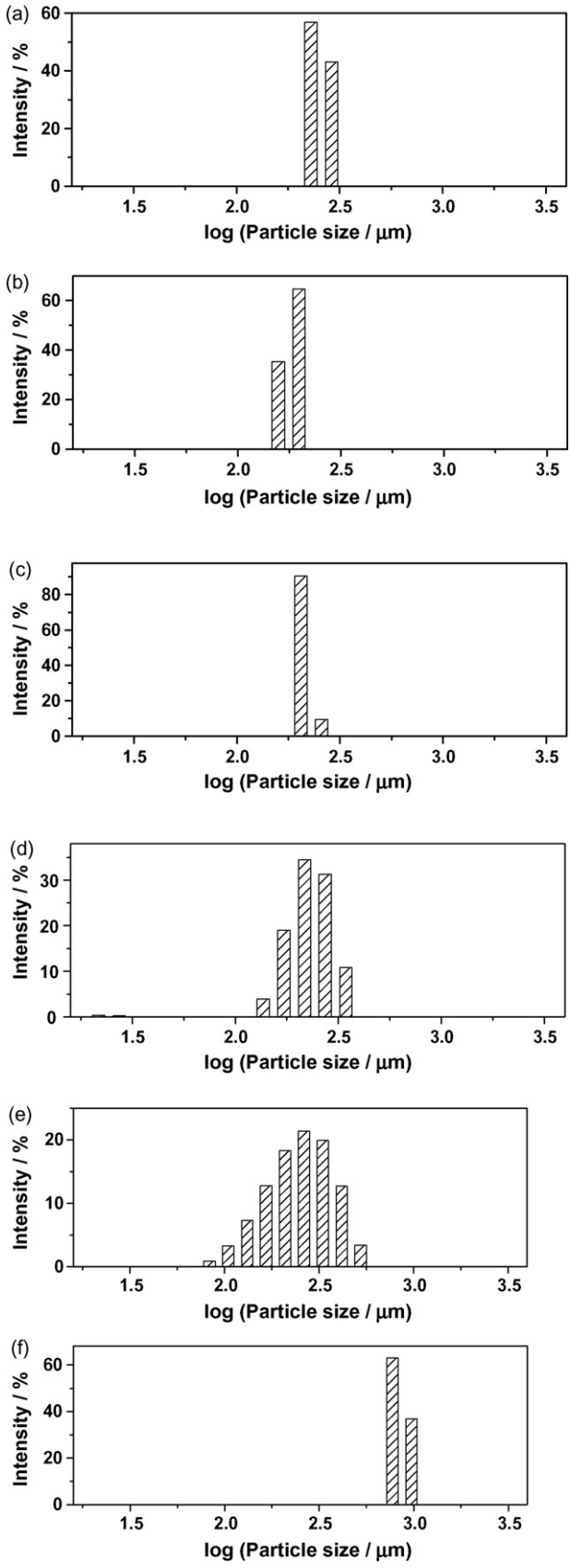

Fig. 2. Particle size distribution of PTFE water dispersion system dispersed in DI water and ethanol measured by DLS. (a) E1 in DI water, (b) E1 in ethanol, (c) E3 in ethanol, (d) E4 in ethanol, (e) E5 in ethanol, and (f) Nafion ionomer in ethanol.

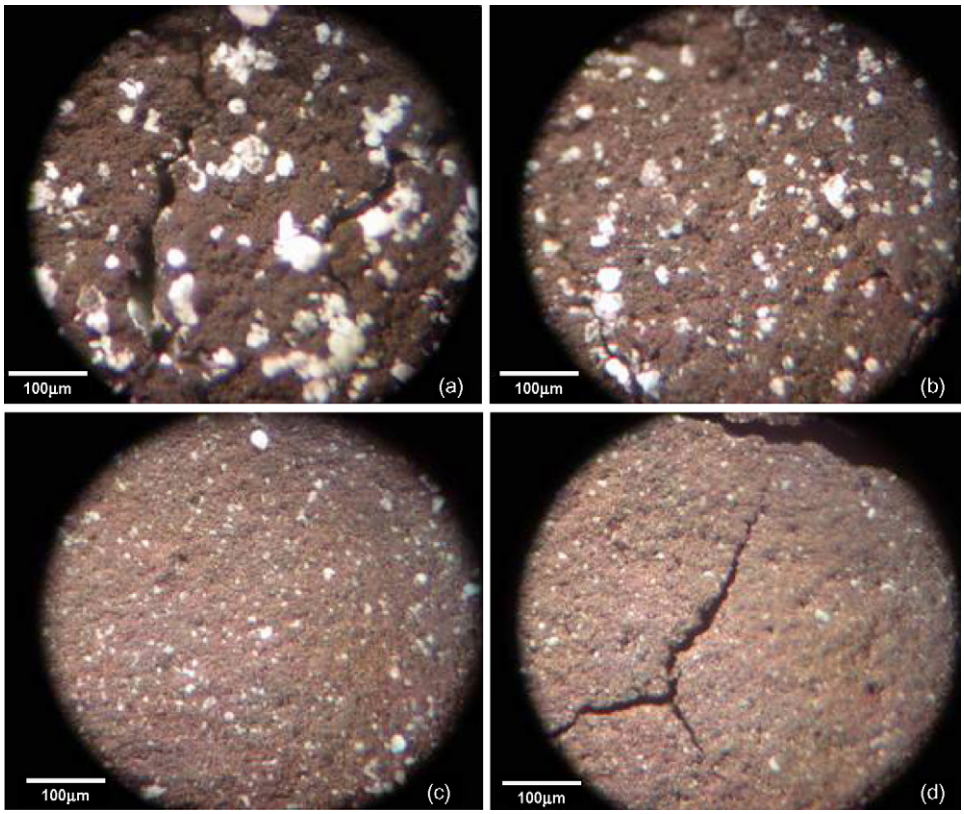

Fig. 3. Surface morphology of dried MPL ink on the slide. (a) MPL prepared with E1, (b) MPL prepared with E3, (c) MPL prepared with E4, and (d) MPL prepared with E5.

3.2. Structure characterization of the diffusion layers with hyperdispersant

Fig. 3 presents the surface morphologies of the dried MPL inks prepared with dispersion E1, E3–E5. As shown in Fig. 3(a), the huge macroscopic agglomerates of the PTFE separate out for the one prepared with E1. Fig. 3(b) and (c) shows the surface morphologies of the MPL inks with different Nafion contents. It is obvious that the particle size of the PTFE in the MPL decreases with the increase in Nafion content. Therefore, the fluorocarbon chain of the Nafion ionomer does provide a stable steric barrier around PTFE particles to reduce the agglomeration behavior of PTFE in MPL inks.

Both Fig. 4 and Table 1 show the gas permeability in the through-plane direction for the fabricated GDLs. In Fig. 4, it can be seen that GDL2 (i.e. the one employing the PTFE dispersion with 1% Nafion content) shows the highest gas permeation velocity at the same pressure gradient. However, with further increase in Nafion content, the gas permeation velocity of the GDL decreases seriously. Considering the thickness in the through-plane direction, the detail gas permeability coefficients of the GDLs are listed in Table 1. While the same trend of the gas permeability coefficient is obtained comparing with the above permeation velocity of the GDLs.

Fig. 5 shows the detailed pore radius distributions curves of GDL1–GDL4. It can be distinguished that GDL2 presents slight loss of pore volume in radius range of 3–4 μm compared with GDL1. However, it is apparent that excessive Nafion in the PTFE dispersion system results in the volume loss of pores in micron scale severely. GDL2 and GDL3 show obvious pore volume loss in radius range of more than 0.7 μm and 0.3 μm, respectively. Table 1 also shows the mercury intrusion volume of the GDLs in specific pore radius range and that in the whole pore radius range. It can be seen that the pore volume in radius range of 0.050–1 μm occupies more than 65% of the total pore volume in the GDL. The additional Nafion ionomer in proper content can increase the pore volume in radius range of 0.050–1 μm, which leads to the total pore volume increase in the GDL. But

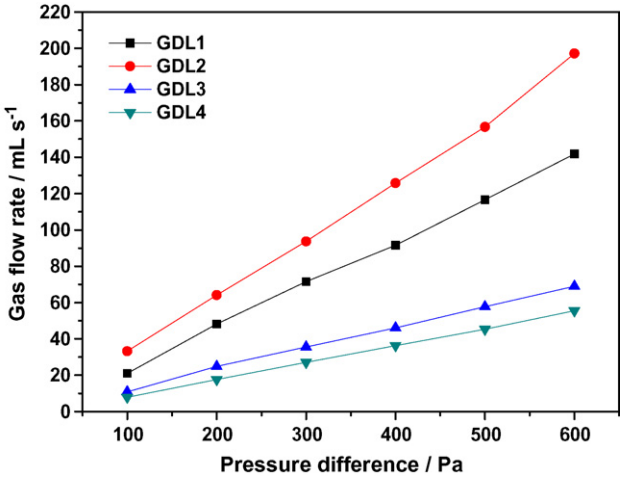

Fig. 4. Gas permeability of the GDL1–GDL4 in through-plane direction.

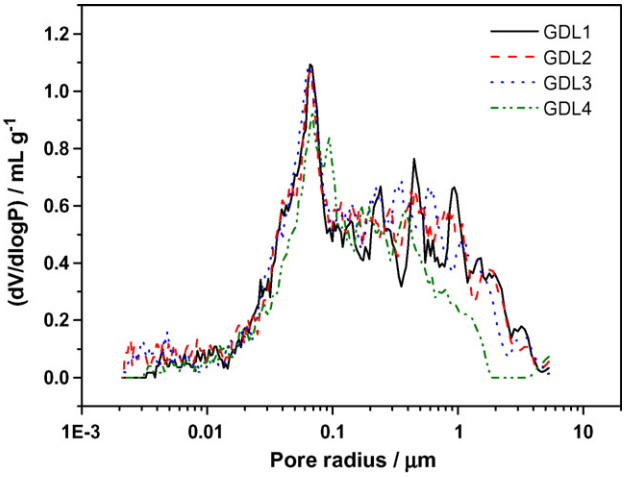

Fig. 5. Pore size distribution of the GDL1–GDL4.

excessive Nafion employed in the PTFE dispersion system leads to the volume loss of the pores in radius range of 0.050–1 μm and total pore volume reduce consequently. As for the larger pores in the GDL, it is obvious that the mercury intrusion volume of the GDL in the radius larger than 1 μm decreases with the increased Nafion content employed in.

William et al. [15] depicted the relationship between the pore structure and the gas permeation of the GDL. It is suggested the higher permeability is attributed to the larger pores, whose size is one hundred times bigger than the mean-free path of air or 3.5 μm in radius. In contrast to this assumption, GDL2 has smaller pore volume in radius range larger than 1 μm comparing with GDL1, but higher gas permeation rate in through-plane direction, which indicates that the pore size distribution is not the only determination factor which can influence the gas permeation in the GDL. Decreased PTFE particle size in GDL not only can increase the packing density of the MPL, but also can improve the crosslink status of the pore and the carbon power themselves in the MPL. That is to say, it can decrease the space enwrapped with PTFE completely, where local gas block and insulation would appear in MPL. Consequently, the increased gas permeation for GDL2 should be attributed to the improvement of the crosslink status of the pore in the GDLs. However, with the increase in the Nafion content further, volume loss of the macropores, whose radius is larger than 0.7 μm for GDL3 and 0.3 μm for GDL4, became the main influential factor to determine the gas permeability.

3.3. Performance variation in DMFC employing different cathode GDLs

The measured internal resistances of cell C1–C4 are 251.6 mΩ cm^2, 222.1 mΩ cm^2, 210.2 mΩ cm^2 and 198.3 mΩ cm^2, respectively. It can be seen that it decreases with the increase in the Nafion content adopted in the cathode GDL. As we employing the same anode, the electrolyte membrane and the cathode catalyst layer in all the cases, the difference of the internal resistance relies on the electronic resistance of the cathode GDLs. Table 1 shows the electronic resistance of the GDLs with different Nafion contents. It is shown that it does decrease with the increase in the Nafion content. The enhancement of crosslink of carbon powder in the MPL is probably the reason for the electronic resistance decreasing.

Fig. 6 shows the curves of the cell performance and the IR corrected anode and cathode polarization curves. It can be distinguished that cell C2 presents the highest cell performance when the cell voltage is above 0.4 V. Compared with cell C1, the additional Nafion ionomer in cathode GDL decreases the cell performance in the range of high-discharging current densities. And it is obvious that the mass transport polarization of cell C2–C4 was the reason for the cathode performance loss. As shown from the IR corrected cathode polarization curves, cell C2–C4 present their obvious cathode mass transport overpotential at 0.22 A cm^{-2}, 0.14 A cm^{-2} and 0.16 A cm^{-2}, respectively.

According to the analysis of TG-MS reported by Zhai et al. [22], Nafion only partly losses its hydrophilic properties in the heat treatment process at 340 °C. Inevitably, the additional hyperdispersant of Nafion ionomer leads to hydrophobic loss in the GDLs. Although the surface contact angle cannot represent the wetting phenomena of the pores in GDL [23], it could be however used for an internal comparison of hydrophobic/hydrophilic properties in the GDL pores basing on the same preparation method. As shown in Table 1, the surface contact angle of the prepared GDLs decreases with the increase in the Nafion content.

As we know, the differences in porosity and the hydrophobic/hydrophilic properties in the cathode GDL result in different two-phase flows and mass transport characteristics. GDL1 and GDL2 have similar pore size distribution and porosity as shown in Fig. 5 and Table 1. According to the suggestion of Pasaogullari and Wang [5], the liquid saturation increases with the decrease in the contact angle under the same porosity. The liquid saturation in GDL2 is therefore higher than GDL1 at same wetting conditions. Consequently, although the GDL2 has higher gas permeability than GDL1, cell C2 shows relatively low cathode limiting current density.

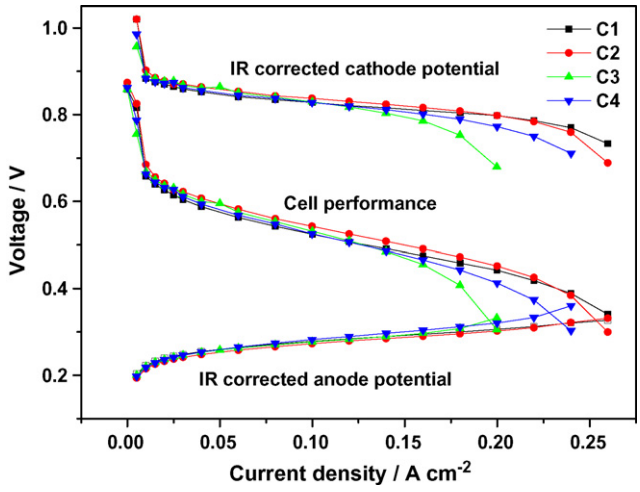

Fig. 6. Cell performance and IR corrected anode and cathode polarization of the cell C1–C4.

As for GDL3 and GDL4, the increased oxygen transfer resistance in the GDL contributes more to the increased mass transfer overpotential for cell C3 and C4. According to the understanding of Lin and Van Nguyen [1] and Park et al. [8], increased mass transport resistance, especially for the liquid water transport, make the cathode catalyst layer suffer flooding, which inhibits oxygen diffusion. Compared with GDL4, GDL3 has more volume of pores in micron scale and more hydrophobic pore for larger surface contact angle and less Nafion addition, which leads to higher capillary force in the interface of the GDL and catalyst layer as well as the higher liquid water transport resistance from the catalyst layer to the GDL in consequence. Therefore, increased oxygen transfer resistance and probably more serious flooding in the cathode catalyst layer make cell C3 present the highest mass transport overpotential in the cathode.

As learned from the above discussion, the cell performance improvement of cell C2 is attributed to the proper Nafion content adopted in the cathode MPL. Nafion ionomer, as a kind of hyperdispersant, can enhance the crosslink of carbon powder and pores themselves simultaneously in the MPL. The enhanced crosslink of carbon powder leads to the electronic resistance decrease. Under the condition of similar pore distribution and porosity, the increased crosslink of pores can decrease the gas transfer resistance of the GDL, which results in the cathode performance being improved. However, excessive Nafion ionomer adopted in the MPL leads to the loss of hydrophobicity and volume of the pores in the micron scale, which blocks the gas transport in the GDL. Because both the high-voltage and high-fuel efficiency operation is desirable for actual DMFC application [24], the GDL made from the MPL ink with 1 wt.% additional Nafion ionomer shows its high-cell performance between 0.55 V and 0.4 V, which displays its advantage as the cathode diffusion layer under ambient conditions.

4. Conclusion

In the prepared process of the cathode MPL ink, it has been shown experimentally that an addition of Nafion ionomer to PTFE water dispersion system leads to decreased particle size of PTFE in the MPL. This finding is owned to the dispersion effect of Nafion ionomer on the PTFE in nonaqueous solvent. Nafion ionomer, as a kind of hyperdispersant, was confirmed to have the ability of reducing the agglomeration behavior of PTFE in ethanol.

Comparative studies were then carried out on the GDLs prepared with the PTFE water dispersion system with different Nafion content. It is shown that, with the increase in the Nafion content, gradually decreased PTFE particle size and increased hydrophobic property loss in the MPL were both achieved. The decreased particle size of PTFE in the MPL not only results in the improved crosslink of carbon and pores themselves, but also leads to the volume loss of the pore whose radius is larger than 0.7 μm for the GDL with 2% Nafion addition and 0.3 μm for that with 5% Nafion addition. As the cathode GDL, the one employing the PTFE dispersion system with 1% Nafion content shows its advantages in the aspect of gas permeability and electronic conductivity.

Acknowledgements

This work was supported by the Hi-Tech Research and Development Program of China (2006AA05Z137, 2006AA05Z139).

References

[1] G.Y. Lin, T. Van Nguyen, J. Electrochem. Soc. 152 (2005) A1942.
[2] H.K. Kim, J.M. Oh, J.H. Kim, H. Chang, J. Power Sources 162 (2006) 497.
[3] Z.G. Qi, A. Kaufman, J. Power Sources 109 (2002) 38.
[4] J.H. Nam, M. Kaviany, Int. J. Heat Mass Transfer 46 (2003) 4595.
[5] U. Pasaogullari, C.Y. Wang, Electrochim. Acta 49 (2004) 4359.
[6] G.Y. Lin, T. Van Nguyen, J. Electrochem. Soc. 153 (2006) A372.
[7] A.Z. Weber, J. Newman, J. Electrochem. Soc. 152 (2005) A677.
[8] S. Park, J.W. Lee, B.N. Popov, J. Power Sources 163 (2006) 357.
[9] E. Passalacqua, G. Squadrito, F. Lufrano, A. Patti, L. Giorgi, J. Appl. Electrochem. 31 (2001) 449.
[10] G.G. Park, Y.J. Sohn, S.D. Yim, T.H. Yang, Y.G. Yoon, W.Y. Lee, K. Eguchi, C.S. Kim, J. Power Sources 163 (2006) 113.
[11] C.S. Kong, D.Y. Kim, H.K. Lee, Y.G. Shul, T.H. Lee, J. Power Sources 108 (2002) 185.
[12] L. Giorgi, E. Antolini, A. Pozio, E. Passalacqua, Electrochim. Acta 43 (1998) 3675.
[13] E. Antolini, R.R. Passos, E.A. Ticianelli, J. Appl. Electrochem. 32 (2002) 383.
[14] J. Moreira, A.L. Ocampo, P.J. Sebastian, M.A. Smit, M.D. Salazar, P. del Angel, J.A. Montoya, R. Perez, L. Martinez, Int. J. Hydrogen Energy 28 (2003) 625.
[15] M.V. Williams, E. Begg, L. Bonville, H.R. Kunz, J.M. Fenton, J. Electrochem. Soc. 151 (2004) A1173.
[16] R.B. Bird, W.E. Stewart, E.N. Lightfoot, Transport Phenomena, John Wiley & Sons, New York, 1960, p. 150.
[17] Q. Mao, G. Sun, S. Wang, H. Sun, G. Wang, Y. Gao, A. Ye, Y. Tian, Q. Xin, Electrochim. Acta 52 (2007) 6763.
[18] T.P. Concannon, in DU PONT DE NEMOURS & CO (Ed.), US4425448-A (1982).
[19] T.R. Gu, P.A. Galera-Gomez, Colloids Surf. A 147 (1999) 365.
[20] J.D. Schofield, Prog. Org. Coat. 45 (2002) 249.
[21] L.G. Lage, P.G. Delgado, Y. Kawano, J. Therm. Anal. Calorim. 75 (2004) 521.
[22] Y.F. Zhai, H.M. Zhang, J.W. Hu, B.L. Yi, J. Membr. Sci. 280 (2006) 148.
[23] V. Gurau, M.J. Bluemle, E.S. De Castro, Y.M. Tsou, J.A. Mann, T.A. Zawodzinski, J. Power Sources 160 (2006) 1156.
[24] X. Ren, P. Zelenay, S. Thomas, J. Davey, S. Gottesfeld, J. Power Sources 86 (2000) 111.